The Cryosphere Discuss., 3, 995–1022, 2009
www.the-cryosphere-discuss.net/3/995/2009/

The Cryosphere
Discussions

A sea ice thickness retrieval model for 1.4 GHz radiometry and application to airborne measurements over low salinity sea ice

L. Kaleschke[1], **N. Maaß**[1], **C. Haas**[2], **S. Hendricks**[3], **G. Heygster**[4], **and R. T. Tonboe**[5]

[1]Institute of Oceanography, University of Hamburg, Bundesstraße 53,
20146 Hamburg, Germany
[2]Department of Earth & Atmospheric Sciences, University of Alberta Edmonton,
Alberta T6G 2E3, Canada
[3]Alfred Wegener Institute for Polar and Marine Research, Bussestr. 24,
27570 Bremerhaven, Germany
[4]Institute of Environmental Physics, University of Bremen, P.O. Box 330440, Germany

[5] Center for Ocean & Ice, Danish Meteorological Institute, Lyngbyvej 100,
2100 Copenhagen, Denmark

Received: 19 October 2009 – Accepted: 6 November 2009 – Published: 18 November 2009

Correspondence to: L. Kaleschke (lars.kaleschke@zmaw.de)

Published by Copernicus Publications on behalf of the European Geosciences Union.

Abstract

In preparation for the European Space Agency's (ESA) Soil Moisture and Ocean Salinity (SMOS) mission we investigated the potential of L-band (1.4 GHz) radiometery to measure sea ice thickness.

Sea ice brightness temperature was measured at 1.4 GHz and ice thickness were measured along nearly coincident flight tracks during the SMOS Sea-Ice campaign in the Bay of Bothnia in March 2007. A research aircraft was equipped with the L-band Radiometer EMIRAD and coordinated with helicopter based electromagnetic induction (EM) ice thickness measurements.

We developed a three layer (ocean-ice-atmosphere) dielectric slab model for the calculation of ice thickness from brightness temperature. The dielectric properties depend on the relative brine volume which is a function of the bulk ice salinity and temperature.

The model calculations suggest a thickness sensitivity of up to 1.5 m for low-salinity (multi-year or brackish) sea ice. For Arctic first year ice the modeled thickness sensitivity is roughly half a meter. It reduces to a few centimeters for temperatures approaching the melting point. Although the campaign was conducted under such unfavorable melting conditions and despite limited spatial overlap between the L-band and EM-measurements was small we demonstrate a large potential for retrieving the ice thickness in the range of 0.2 to 1.5 m.

Furthermore, we show that the ice thickness derived from SMOS measurements would be complementary to ESA's CryoSat-2 mission in terms of the error characteristics and the spatio-temporal coverage.

1 Introduction

Soil Moisture and Ocean Salinity (SMOS) is an earth observation mission developed by the European Space Agency (ESA) launched on 2 November 2009. NASA's Aquarius mission is planned to follow in 2010. Their main objectives are to provide global measurements of soil moisture over land and sea surface salinity over ocean from L-band (ν=1.4 GHz, λ=21 cm) radiometric observations. An exciting spin-off is the retrieval of sea ice thickness which was expected to be possible due to the large penetration depth at L-band (Mätzler, 2001). These new L-band radiometers could provide sea ice thickness information complementary to that from altimeters because of the expected sensitivity to thin ice thickness variations. Moreover, they would provide near real time data with an almost global coverage every second day which is important for operational applications such as weather prediction and ship routing. Thin ice in the 0- to 0.4-m range dominates the ocean-atmosphere heat exchange in the Arctic during the cold months (Maykut, 1978) and is important for the large-scale sea ice rheology (Feltham, 2008).

Menashi et al. (1993) have demonstrated the possibility of ice thickness retrieval for radiometric measurements at 0.6 GHz. In this article we describe the adaption of their model for the conditions encountered in the Baltic Sea. The model will be used for the analysis of L-band radiometric and EM ice thickness measurements which were obtained in the Bothnian Bay in March 2007 as part of the first SMOS sea ice campaign.

The Microwave Imaging Radiometer using Aperture Synthesis (MIRAS), the SMOS payload, is based on a novel technique for passive microwave aperture synthesis inspired from radio astronomy (Corbella et al., 2004). MIRAS measures not the brightness temperature of the scene, but its Fourier spectrum by the correlation of 69 individual antennas. The inversion of the spectrum leads to a field of view with hexagon-like shape and a nadir resolution of about 35 km. The MIRAS swath width is about 1000 km. A discussion of the spatial accuracy of the SMOS sea ice thickness retrieval is beyond the scope of this paper.

The specific aim of this study is the investigation of thermal microwave radiation emitted by a homogeneous closed ice cover at 1.4 GHz. We try to answer the following questions: how can we measure ice thickness from the observed brightness temperature, in which range, and with what accuracy? How are the results influenced by the ice temperature and salinity? Will there be an advantage of SMOS compared to CrySat-2 for sea ice thickness measurement?

There are only very limited validation data available for this purpose. The only measurements of the 1.4 GHz brightness temperature together with the ice thickness were obtained in the Baltic Sea during the SMOS Sea-Ice field campaign in the mild March 2007. For this reason we restrict the discussion to low salinity ice at high temperatures which was observed during this particular field campaign. However, the model presented in the following could be applied for the Arctic and Antarctic as well. As the model is designed for retrieval, we have to make a number of simplifications to reduce the number of free parameters. A comparison with models of higher complexity has been conducted in the framework of the ESA SMOS-Ice project and is covered in the final report (Heygster et al., 2009).

2 Emissivity model for 1.4 GHz

In our model we assume only two surface types, open water and ice with the fractional area coverage (total ice concentration) $1-C$ and C, respectively. The observed brightness temperature at the surface depends on the temperatures of water T_{water} and ice T_{ice} and their emissivities e_{water} and e_{ice}. Furthermore, T_{obs} is a function of the incidence angles and the polarisation but we will restrict our discussion to the nadir case without loss of generality.

$$T_{\text{obs}} = (1-C)e_{\text{water}}T_{\text{water}} + Ce_{\text{ice}}T_{\text{ice}} \qquad (1)$$

We here neglect the atmospheric contribution, ionospheric effects, cosmic and solar radiation (Reul et al., 2008; Tenerelli et al., 2008). The latter terms are of importance for sea surface salinity retrieval with demanding requirements on the radiometer's accuracy. However, all terms are relatively small compared to the large brightness contrast between water and thick ice which cover a 150 K range from 90 K to 240 K. For sea surface salinity retrieval one has to utilise a much narrower range covering only a few K or even tenths of a K.

In the following we limit the discussion to a closed ice cover with $C \approx 1$. The question remains open if simultaneous retrieval of ice concentration and thickness retrieval will be possible with SMOS data alone. However, with the model described in the following we see no possibility for simultaneous retrieval even by taking different polarisations and incidence angle into account (Kaleschke and Maaß, 2009). Thus, it is necessary to prescribe the ice concentration which can be well done by using data from other sensors.

2.1 Open water

The emissivity of the water surface e_{water} is calculated from the Fresnel equations (Swift, 1980). We apply the model of Klein and Swift (1976) for the permittivity of sea water. The nadir brightness temperature of the ocean surface close to the freezing point is 92±1 K for salinities between 33 and 35, e.g. in the Arctic marginal ice zone, and 96±1 K in the northern Baltic Sea where surface salinities range between 2 and 7 (Leppäranta and Myrberg, 2009). At L-band the sensitivity of wind induced surface roughness is as small as 0.2 K per 1 m/s (Dinnat and Boutin, 2003). Thus, the wind influence can certainly be neglected for the aim of sea ice thickness retrieval.

2.2 Sea ice emissivity

Brine pockets and air bubbles are much smaller than the L-band wavelength of 21 cm. Therefore, the sea ice can be considered as a homogeneous medium which greatly simplifies the set-up of an emissivity model at 1.4 GHz. The emissivity of ice e_{ice} follows from considering reflection at a dielectric slab of ice over water. The reflection coefficient of an ice slab over an infinite half plane can be expressed as a function of the reflection coefficients R_1 and R_2, describing reflection at the upper and lower boundary of the slab (Ulaby et al., 1981):

$$R = \frac{R_1 + R_2 e^{-2ik_{i,z}d}}{1 + R_1 R_2 e^{-2ik_{i,z}d}} \tag{2}$$

where d is ice thickness and $k_{i,z}$ is the z-component of the propagation vector in ice $\boldsymbol{k_i}$, with the z-axis perpendicular to the slab. The expression for $k_{i,z}$ can be separated into its real part β, which is called the phase constant, and its imaginary part α, which is referred to as the attenuation coefficient: $k_{i,z} = \beta - i\alpha$. The expressions for α and β are

$$\alpha = \frac{\omega}{c_0}\cos\theta_i |Im\sqrt{\epsilon_i}| \tag{3}$$

$$\beta = \frac{\omega}{c_0}\cos\theta_i Re\sqrt{\epsilon_i} \tag{4}$$

with the angle of refraction θ_i in the ice, the relative permittivity of ice ϵ_i, the angular frequency $\omega = 2\pi f$, and the speed of light c_0 in vacuum. The ice emissivity is calculated from $e_{ice} = 1 - r = 1 - R\overline{R}$, where r is reflectivity and $\overline{R}$ is the conjugate-complex of the reflection coefficient R. Assuming real power reflection coefficients the following expression for ice emissivity was derived (Menashi et al., 1993):

$$e_{ice} = \frac{(1 - r_i)(1 - Ar_w)}{1 + Ar_i r_w + 2\sqrt{Ar_i r_w}\cos(2\beta d)} \tag{5}$$

where $A = \mathrm{e}^{-4\alpha d}$. The reflectivity of air to ice r_i and the reflectivity of ice to water r_w are calculated from the Fresnel equations with the permittivity of ice provided in the next section.

The above equation is a coherent solution describing ice emissivity as a periodic function of ice thickness. If the rms thickness variation of the ice slab is sufficiently large, i.e. more than a quarter of the used electromagnetic wavelength over the illumination footprint, the periodicity averages out and an incoherent solution can be introduced instead. The emissivity of ice averaged over a variety of ice thicknesses was derived by Menashi et al. (1993) and can be expressed as follows:

$$e_{\mathrm{ice}} = \frac{(1 - r_i)(1 - Ar_w)}{1 - Ar_i r_w}\left[\frac{1 - \sqrt{Ar_i r_w}\mathrm{e}^{-\beta\sigma_\mathrm{d}}}{1 + \sqrt{Ar_i r_w}\mathrm{e}^{-\beta\sigma_\mathrm{d}}}\right] \tag{6}$$

Title Page
Abstract
Introduction
Conclusions
References
Tables
Figures
◀︎|
|▶︎
◀︎
▶︎
Back
Close
Full Screen / Esc
Printer-friendly Version
Interactive Discussion

where σ_d is rms thickness variation (roughness). The equations presented in Menashi et al. (1993) contain the optical pathlength l and its variation σ_l instead of ice thickness d and thickness variation σ_d in Eq. (6). This is a small mistake of Menashi et al. (1993) and contradictory to Ulaby et al. (1981). The expressions for the attenuation coefficient α and the phase coefficient β used by Menashi et al. (1993) do not take into account the cosine term, which originates from considering the z-component of the propagation vector only (Eqs. 3, 4). However, this mistake has only a minor effect and the scientific results obtained by Menashi et al. (1993) remain unquestioned.

The transition of open water to a very thin ice cover falls outside the assumptions for the incoherent solution. However, we assume that a smooth connection of the open water emissivity and the valid part of the model is a reasonable assumption.

2.2.1 Sea ice permittivity

Vant et al. (1978) proposed an empirical relationship for the permittivity of ice depending on the relative brine volume (in ‰; valid for $V_b < 70‰$):

$$\epsilon_{\text{ice}} = a_1 + a_2 V_b + i(a_3 + a_4 V_b) \tag{7}$$

In this study a linear combination of the coefficients derived at 1 and 2 GHz (Table 1) is used as an approximate value for 1.4 GHz. Leppäranta and Manninen (1988) derived equations for determining the relative brine volume for low-salinity ice with temperatures between −2°C and 0°C

$$V_b = \frac{\rho_i S_{\text{ice}}}{F_1(T) - \rho_i S_{\text{ice}} F_2(T)}. \tag{8}$$

Table 2 gives the coefficients of the polynomials $F = \sum_{j=0}^{3} \alpha_j T^j$. The pure ice density ρ_i is 917 kg/m^3. Winter bulk ice salinity averaged over samples collected at landfast sea ice in the Gulf of Finland in 1999–2001 is $S_{\text{ice}} = 0.65 \pm 0.3$ (Granskog et al., 2004). For more saline ice and lower temperatures the equations of Cox and Weeks (1983) and Frankenstein and Garner (1967) are applied instead.

3 Measurements

The brightness temperature at 1.4 GHz was measured in the Bothnian Bay in March 2007. The Helsinki University of Technology (HUT) SkyVan research aircraft was equipped with the Technical University of Denmark (DTU) National Space Institute Radiometer (EMIRAD). The non-imaging EMIRAD measurements were coordinated with helicopter EM ice thickness measurements on 12 and 13 March. The air temperature measured at Hailuoto increased from an average of −6°C on the 5 March to an average above 0°C on 12 and 13 March. Photographs taken during the flights show features that look like a very wet surface or even like ponded ice (Fig. 4).

3.1 L-band radiometer EMIRAD

EMIRAD measures the fully polarimetric state of the electromagnetic emission (Rotbøll et al., 2003). The radiation was measured with two antennas, one with a nadir beam and the other with an aft looking beam with an angle of incidence of 40°. The footprint of the nadir measurement at a flight level of 1000 m is about 680 m. The radiometer data were provided with a sampling rate of 125 Hz. The signal was integrated over 200 samples leading to a oversampled footprint spacing of approximately 90–100 m.

The EMIRAD data was seen to be occasionally degraded due to unstable behavior of the power converter. This caused deviations from the nominal performance of the radiometer and introduced spikes and jumps in the data. The brightness temperature signals were carefully investigated and obviously degraded sections were removed from the analysis.

3.2 Electromagnetic induction system

A system of a transmitter and receiver coil operating at 3.68 kHz is used to estimate sea ice thickness (Haas et al., 2009). The footprint of a single measurement is about 40 m, while the recording frequency of 10 Hz results in a point spacing of 3–4 m at typical speeds of a helicopter. The general accuracy over level ice is ±10 cm. Over ridged areas the error can increase to about 50% of ice thickness. Additional errors can arise in shallow brackish waters (Haas, 2004; Hendricks and Haas, 2009).

4 Results

4.1 Model sensitivity study

The modeled brightness temperature mainly depends on polarisation, incidence angle, ice concentration, ice thickness, ice and water salinities, ice and water temperatures, and sea ice roughness. We here restrict the investigation to the nadir ice thickness retrieval for ice concentration near 100%. The most important free parameters are the ice and the water salinity and temperature, as well as the ice roughness. In the following we keep the water salinity and temperature fixed at $S_{\text{water}} = 2$ and $T_{\text{water}} = 0^{\circ}$C, and vary the ice roughness, temperature and salinity.

4.1.1 Sea ice roughness

The sea ice roughness σ_d influences the asymptotic behavior of the emissivity model towards zero ice thickness. The resulting emissivities for different parameterizations of σ_d are shown in Fig. 1. The coherent solution for the emissivity of a plane-parallel ice slab over an infinite half plane reduces to the emissivity of open water for a vanishing ice thickness. The incoherent form (Eq. 6) with a parameterization of σ_d as a fixed percentage of ice thickness also approaches the emissivity of open water. The incoherent solution for a constant positive σ_d does not converge to the emissivity of open water. In the following the parameterization $\sigma_d = 0.1d$ is used with the incoherent model.

4.1.2 Sea ice temperature and salinity

The resulting brightness temperatures for different sea ice bulk temperatures and salinities are shown in Fig. 2. For Baltic sea ice with $S = 0.65$ the brightness temperature levels out at about $d = 0.5$ m for $T_{\mathrm{ice}} = -0.5^{\circ}$C and at $d = 1.5$ m for $T_{\mathrm{ice}} = -2^{\circ}$C. For $T_{\mathrm{ice}} = -3^{\circ}$C the penetration depth is approximately 1.5 m for these low salinity conditions. For typical Arctic or Antarctic first year ice with $T_{\mathrm{ice}} = -5^{\circ}$C and $S = 8$ the resulting brightness temperature (not shown) resembles that of the Baltic sea ice at $T_{\mathrm{ice}} = -0.5^{\circ}$C.

4.2 A semi-empiric retrieval model

Several relatively simple empiric or semi-empiric models have been successfully applied for the retrieval of sea ice concentration from passive microwave sensors (Andersen et al., 2007). The inverse retrieval problem is in general ill-posed. The following simplifications are a way to constrain the inverse problem with a priori knowledge namely the assumption about sea ice concentration, temperature and salinity. In the following we describe a semi-empiric formulation that could later be used for the satellite retrieval.

An approximation of the emissivity model (Eqs. 1, 6) is given by the following expression

$$T_{\mathrm{obs}} = T_m - (T_m - T_0)\exp(-\gamma d), \tag{9}$$

with the brightness temperature of open water T_0 and an attenuation factor γ. The mixture brightness temperature T_m is defined as

$$T_m = CT_1 + (1 - C)T_0, \tag{10}$$

with the brightness temperature of infinitely thick ice T_1 and ice concentration C.

The three fit parameters T_0, T_1, and γ can be obtained either from an emissivity model or from satellite and field data. For satellite applications, the parameters T_0 and

T_1 could be estimated from minimum and maximum values of the observed brightness temperature if there is a completely ice-free and a thick ice-covered footprint in the swath. The coefficient γ could be estimated once for a specific region and season by the means of a validation data set that includes the brightness temperatures for different sea ice thicknesses.

The results of the semi-empiric model are shown in Fig. 2 together with the results of the emissivity model. The accuracy of the fit is better than ±1 K for $d > 0.1$ m and $C > 0.5$. Thus, it is a good approximation for the major part of the ice covered seas.

Equation 9 can directly be inverted for the retrieval of ice thickness

$$d = -\frac{1}{\gamma}\ln\left(\frac{T_m - T_{\mathrm{obs}}}{T_m - T_0}\right) \tag{11}$$

The sensitivity of the retrieval to variations in temperature and concentration is shown in Fig. 3. For example, a variation in the ice temperature by ±1°C around a mean temperature of −2°C results in a deviation of ±0.05 m for $d = 0.2$ m ($T_{\mathrm{obs}} = 180$ K), and in a deviation of ±0.1 m for $d = 0.4$ m ($T_{\mathrm{obs}} = 220$ K). An uncertainty in the radiometric accuracy of ±1 K leads to a thickness uncertainty of ±0.02 m for $d = 0.4$ m, and ±0.05 m for $d = 0.7$ m. Errors in the prescribed ice concentration propagate in the same way as errors in the radiometric accuracy whereas a 5% error in the concentration would translate to a 7 K error in the brightness temperature. Thus, a 5% ice concentration error would translate into an uncertainty of ±0.1 m for a thickness of 0.5 m. A 5% error is likely the upper limit of uncertainty for ice concentration retrievals in the central Arctic (Andersen et al., 2007).

The most important error characteristic is defined by the condition $T_{\mathrm{obs}} > T_1$ which defines the maximum ice thickness $d_{\max}$ that can be retrieved. Towards this limit the errors become infinitely large and asymmetric. For Baltic sea ice at $T = -3$°C the maximum thickness is $d_{\max} \approx 1.5$ m for an assumed measurement uncertainty of 1 K. It reduces to 0.9 m for Baltic sea ice at a temperature of $T = -1$°C.

4.3 Comparison of ice thickness retrievals

The campaign dataset consists of four profiles of nearly coincident EM and EMIRAD measurements. The analysis of the data is complicated because of the relatively small EM footprint and the spatial displacement between both measurements. In the following we show the analysis for the flight track with the best spatial overlap of EM and EMIRAD measurements. The vertical channel of the aft looking antenna was heavily degraded for this track. Therefore, we consider the nadir data only.

The sea ice thickness d_{TB} was obtained from the brightness temperature by the inversion of the semi-empiric model (Eq. 11) for a prescribed ice concentration $C = 0.98$, salinity $S_{\mathrm{ice}} = 0.65$, and a ice bulk temperature range $T_{\mathrm{ice}} = -2\pm1^{\circ}\mathrm{C}$. The resulting thickness is shown in Figs. 5 and 6 together with the smoothed and high frequency EM thickness d_{EM}, an ASAR image, and bathymetric data.

Ridged areas and ship tracks that are well visible in the ASAR image are recognized in both thickness retrievals. The darker area in the ASAR image on the right hand side agrees with retrieved thicknesses between 0.2 and 0.5 m. Gaps in the d_{TB} curve indicate a failure of the retrieval which could be either explained by ice temperatures higher than $T_{\mathrm{ice}} = -1^{\circ}\mathrm{C}$ or ice thicker than 1.5 m.

The correlation of d_{EM} and d_{TB} is 0.5 which indicates a relationship which was very likely (99.7% significance) not caused by chance (Fig. 7). The data points shown in Fig. 7 are averages over about 1200 m long sections. The overall mean thickness and the standard deviation of the thickness derived from the EM measurement and from the 1.4 GHz radiometry are $d_{\mathrm{EM}} = 0.82\pm0.4$ m and $d_{\mathrm{TB}} = 0.65\pm0.3$ m, respectively. The results agree with SMHI ice maps that indicate level ice thicknesses in the range of 0.15–0.7 m.

4.4 Complementarity of SMOS and CryoSat ice thickness retrieval

Why could there be a benefit of combining SMOS and CryoSat data? We describe in the following the error characteristics for both sensors.

The CryoSat sea ice thickness retrieval will be based on the measurement of sea ice freeboard. Using a priori information about the snow thickness, and the snow and sea ice densities the freeboard can be converted into a thickness. We assume a ±1 cm uncertainty for the freeboard measurement as the only error source. The SMOS retrieval for Baltic sea ice of $T_{\text{ice}} = -1^{\circ}\text{C}$ shall be influenced by a radiometric uncertainty of ±5 K as the only error source. The resulting relative errors of the retrieval are shown in Fig. 8. It can be seen that below a thickness of about 0.4 m the relative error of the SMOS retrieval is smaller than that of CryoSat. It should be stressed that the results shall be interpreted only qualitatively since the error budget is incomplete and only a very rough estimate. However, the main characteristics will remain similar for a more complete and accurate error budget. The shown complementarity could be exploited in a combined dataset from both sensors. The SMOS data should then be taken into account if the ice is indicated to be thinner than 0.4 m. Assimilation systems like that of Kauker et al. (2009) could take advantage of such input data if the uncertainties are accurately estimated.

5 Conclusions

The new SMOS L-band radiometer was recently launched and NASA's Aquarius mission is awaiting its launch. We described a model for the retrieval of ice thickness from L-band radiometric data. We tested it against aircraft measurements of 1.4 GHz brightness temperature and coincident ice thickness data derived using electromagnetic induction.

The incoherent model solution (Fig. 1) shows a monotonic increase of brightness temperature for increasing ice thickness. This allows calculating the sea ice thickness from the measured brightness temperature by a simple inversion of the function for prescribed free parameters. The model degrees of freedom are limited and the needed information can be obtained from other satellites, e.g. the ice concentration and the ice temperature from AMSR-E, or can be parameterized. The most important model parameters beside incidence angle, ice thickness, and ice concentration are the ice surface roughness, the ice bulk temperature and the ice bulk salinity. Variations in ocean salinity and temperature can be neglected for this application because of the large radiometric contrast between ice and water. A parameterization of the sea ice roughness as a percentage of ice thickness seems to be a reasonable approach. New measurements are necessary to validate this parameterization.

The SMOS Sea-Ice campaign was conducted under adverse melting conditions which lead to a small thickness sensitivity of the ice emissivity. Towards larger ice thickness the retrieval error becomes infinitely large. We suggest, that the retrieval should be interpreted as a lower boundary of the thermodynamic (i.e. modal or level) ice thickness. The retrievable maximum ice thickness is constrained by the ice temperature and salinity.

Overall, this study supports the expectation that the new spaceborne 1.4 GHz radiometers can be used to measure ice thickness. Our model results suggest, that the upper limit for the sea ice thickness retrieval will be roughly half a meter for the Arctic and 1.5 m for the Baltic.

More ice thickness measurements are needed for the validation. The time and position of future validation campaigns is uncritical because of the good spatio-temporal coverage of the SMOS data which is of great advantage as compared to altimeters.

Thin ice plays an important role for heat exchange between the ocean and the atmosphere. Therefore, an ice thickness product based on L-band radiometry will probably be useful for sea ice applications in climate research and meteorology, as well as possibly for ship navigation in polar waters, and would be complementary to the thickness derived from altimetric freeboard measurements.

Acknowledgements. We thank Jan E. Balling and Niels Skou for the provision of the EMIRAD data, Juha Karvonen and Markku Similä (FIMR) for provision of ASAR data, meteorological informations and photographs. We thank Christian Mätzler for discussion. The work was funded by ESA under Contract 21130/08/NL/EL.

References

Andersen, S. Tonboe, R. Kaleschke, L. Heygster, G. and Pedersen, L. T.:Intercomparison of passive microwave sea ice concentration retrievals over the high-concentration Arctic sea ice, J. Geophys. Res, 112, C08004, doi:10.1029/2006JC003543, 2007. 1005, 1006

Corbella, I., Duffo, N., Vall-llossera, M., Camps, A., and Torres, F.:The visibility function in interferometric aperture synthesis radiometry, IEEE T. Geosci. Remote, 42(8), 1677–1682, 2004. 998

Cox, G. and Weeks, W.: Equations for determining the gas and brine volumes in sea-ice samples, J. Glaciol., 29, 306–316, 1983. 1002

Dinnat, E. P. and Boutin, J.: Issues concerning the sea emissvity modeling at L band for retrieving surface salinity, Radio Sci., 38, 8060, doi:10.1029/2002RS002637, 2003. 1000

Feltham, D. L.: Sea Ice Rheology, Annu. Rev. Fluid Mech., 40, 91–112, doi:10.1146/annurev.fluid.40.111406.102151, 2008. 998

Frankenstein G. and Garner, R.: Equations for determining the brine volume of sea ice from −0.5C to −22.9C, J. Glaciol., 6(48), 943–944, 1967. 1002

Granskog, M., Lepparanta, M., Kawamura, T., Ehn, J., and Shirasawa, K.: Seasonal development of the properties and composition of landfast sea ice in the Gulf of Finland, the Baltic Sea, J. Geophys. Res, 109(C2), C02020, doi:10.1029/2003JC001874, 2004. 1002

Hallikainen, M. and Winebrenner, D. P.: The physical basis of sea ice remote sensing, in: Microwave remote sensing of sea ice, edited by: Carsey, F. D., AGU Monograph, 68, Am. Geophys. Union, Washington, DC, 29–46, 1992. 1013

Haas, C.: Airborne EM sea-ice thickness profiling over brackish Baltic sea water, Proceedings of the 17th international IAHR symposium on ice, 21–25 June, 2004, vol. 2, All-Russian Research Institute of Hydraulic Engineering (VNIIG), Saint Petersburg, Russia, 12–17, 2004. 1004

Haas, C., Lobach, J., Hendricks, S., Rabenstein L., and Pfaffling, A.:Helicopter-borne measurements of sea ice thickness, using a small and lightweight, digital EM bird, J. Appl. Geoph., 67(3), 234–241, 2009. 1003

Heygster, G., Hendricks, S., Kaleschke, L., Maaß, N., Mills, P., Stammer, D., Tonboe, R. T., and Haas, C.: L-Band Radiometry for Sea-Ice Applications, Final Report for ESA ESTEC Contract 21130/08/NL/EL, Institute of Environmental Physics, University of Bremen, 2009. 999

Hendricks, S. and Haas, C.: WP 2.2: POL-ICE campaign: Ice thickness observations, in: L-Band Radiometry for Sea-Ice Applications, Final Report for ESA ESTEC Contract 21130/08/NL/EL, 2009. 1004

Kaleschke, L. and Maaß, N.: WP 2.1: Campaign data analysis; WP 2.5: Ice concentration vs. ice thickness, in: L-Band Radiometry for Sea-Ice Applications, Final Report for ESA ESTEC Contract 21130/08/NL/EL, 2009. 1000

Kauker, F., Kaminski, T., Karcher, M., Giering, R., Gerdes, R., and Voßbeck, M.: Adjoint analysis of the 2007 all time Arctic sea-ice minimum, Geophys. Res. Lett., 36, L03707, doi:10.1029/2008GL036323, 2009. 1008

Klein, L. and Swift, C.: An improved model for the dielectric constant of sea water at microwave frequencies, IEEE J. Ocean Eng., OE-2, 104–111, 1976. 1000

Leppäranta, M. and Manninen, T.: The brine and gas contents of sea ice with attention to low salinities and high temperatures, Internal Report 2, Finnish Institute of Marine Research, 1988. 1002, 1014

Leppäranta, M. and Myrberg, K.: Physical oceanography of the Baltic Sea, Springer Verlag, 2009. 1000

Mätzler, C.: Applications of SMOS over terrestrial ice and snow, 3rd SMOS Workshop, DLR, Oberpfaffenhofen, Germany, 10–12 December, 2001. 998

Maykut, G. A.: Energy exchange over young sea ice in the central Arctic, J. Geophys. Res., 83, 3646–3658, 1978. 998

Menashi, J., Germain, K. S., Swift, C., Comiso, J., and Lohanick, A.: Low-frequency passive-microwave observations of sea ice in the Weddell Sea, J. Geophys. Res, 98, 22569–22577, 1993. 998, 1001, 1002

Reul, N., Tenerelli, J., Chapron, B., and Waldteufel, P.: Modeling Sun Glitter at L-Band for Sea Surface Salinity Remote Sensing With SMOS, IEEE T. Geosci. Remote, 45, 2073–2087, 2008. 999

Rotbøll, J., Søbjærk, S. S., and Skou, N.: A novel L-band polarimetric radiometer featuring sub-harmonic sampling, Radio Sci., 38(3), 8046, doi:10.1029/2002RS002666, 2003. 1003

Swift, C. T.: Passive microwave remote sensing of the ocean – a review, Bound. Lay. Meteorol., 18, 25–40, 1980. 1000

Tenerelli, J., Reul, N., Mouche, A. A., and Chapron, B.: Earth-Viewing L-Band Radiometer Sensing of Sea Surface Scattered Celestial Sky Radiation – Part I: General Characteristics, IEEE T. Geosci. Remote, 46, 659–674, 2008. 999

Ulaby, F. T., Moore, R. K., and Fung, A. K.: Microwave remote sensing, active and passive. Volume I: Fundamentals and Radiometry, Addison Wesley Pub., London, UK, 1981. 1000, 1002

Vant, M., Ramseier, R., and Makios, V.: The complex-dielectric constant of sea ice at frequencies in the range 0.1–40 GHz, J. Appl. Phys., 49, 1264–1280, 1978. 1002

Title Page
Abstract
Introduction
Conclusions
References
Tables
Figures
◀▮ ▶▮
◀ ▶
Back
Close
Full Screen / Esc
Printer-friendly Version
Interactive Discussion

Table 1. Coefficients for the calculation of the sea ice dielectric constant (Hallikainen and Winebrenner, 1992).

	a_1	a_2	a_3	a_4
First year ice				
1 GHz	3.12	0.0090	0.039	0.00504
2 GHz	3.07	0.0076	0.034	0.00356
Multi year ice				
1 GHz	3.12	0.0090	−0.004	0.00436
2 GHz	3.07	0.0076	0.013	0.00435

Table 2. Polynomial coefficients for the calculation of the brine volume (Leppäranta and Manninen, 1988).

	α_0	α_1	α_2	α_3
F_1	−0.041221	−18.407	0.58402	0.21454
F_2	0.090312	−0.016111	0.00012291	0.00013603

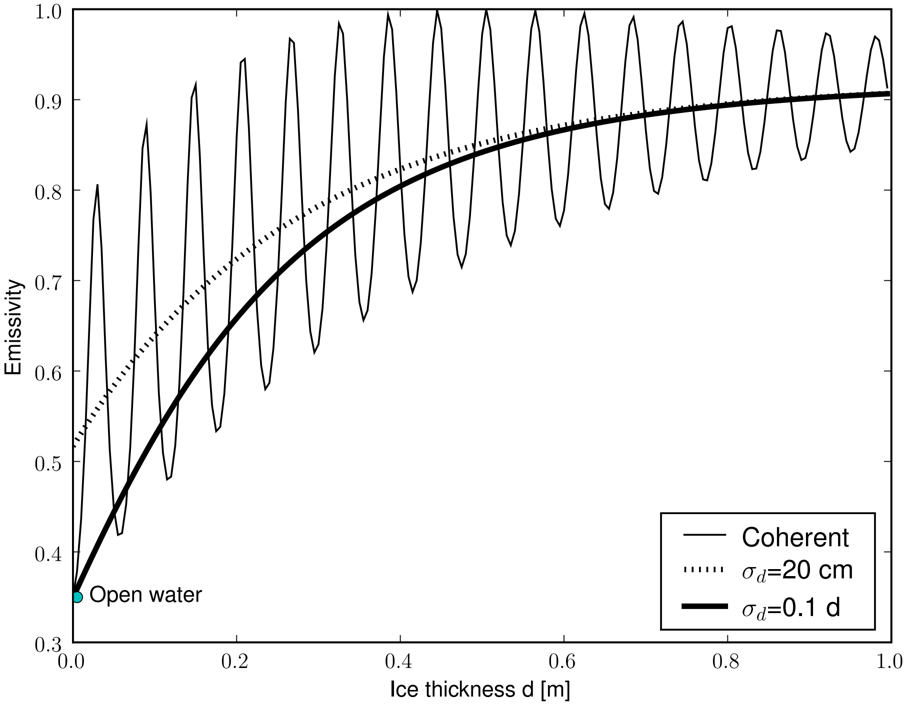

Fig. 1. Nadir 1.4 GHz emissivity of a slab of Baltic sea ice ($S = 0.65$, $T = -2^\circ$C). The coherent and incoherent solution are shown for different parameterizations of the thickness roughness σ_d. The open water emissivity is indicated with the filled circle.

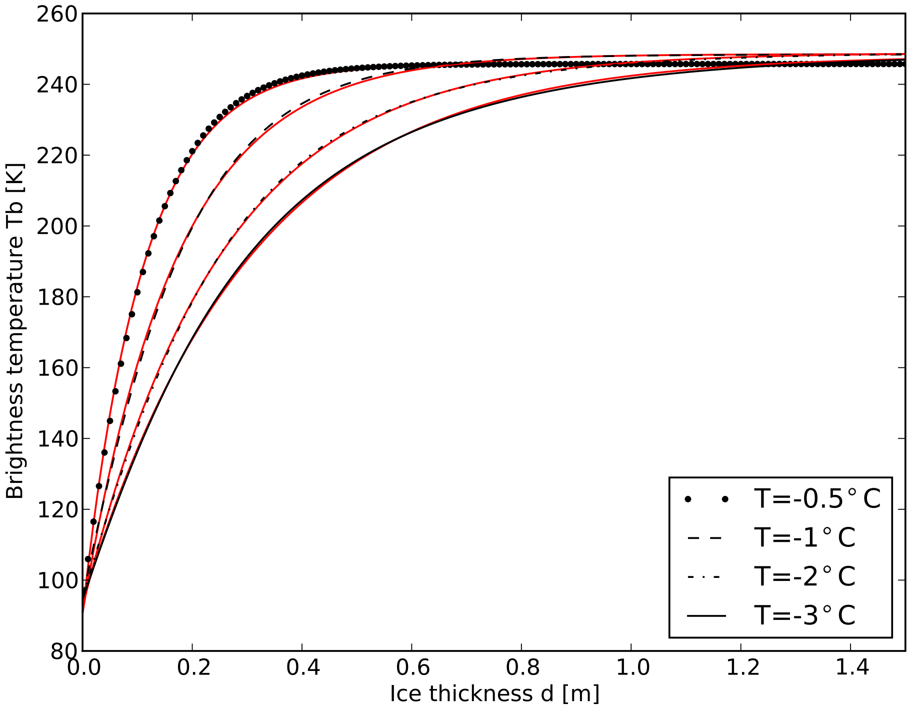

Fig. 2. Nadir 1.4 GHz brightness temperature of Baltic sea ice ($S = 0.65$, roughness $\sigma_d = 0.1d$) for different ice temperatures. The results of the semi-empiric model (Eq. 9) are indicated with the red lines.

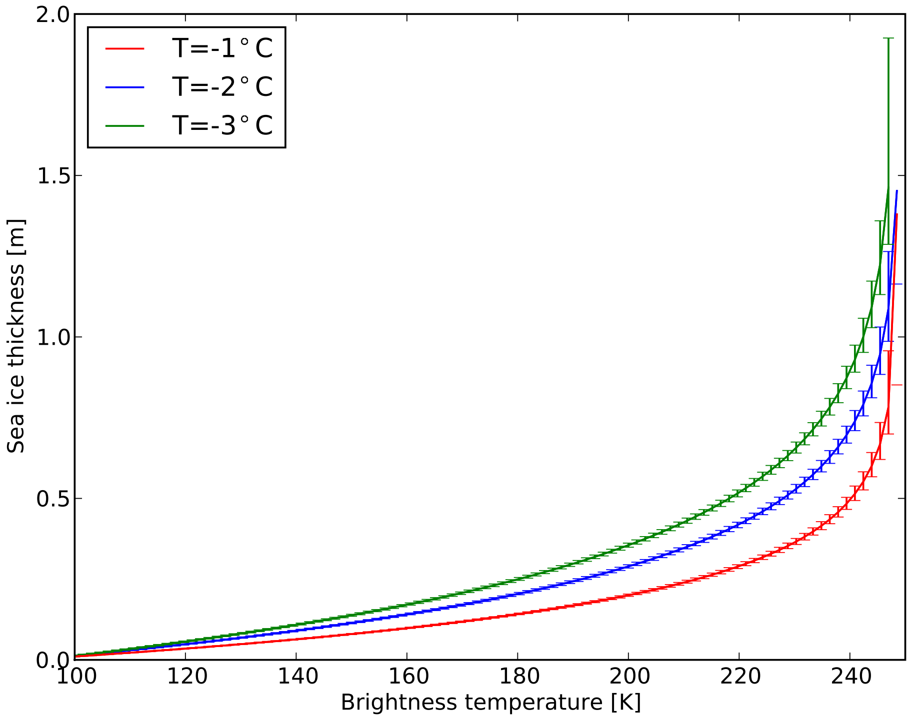

Fig. 3. Model inversion for the retrieval of the ice thickness from the brightness temperature. The error bars indicate ±1 K variations of the brightness temperature.

Fig. 4. Melted surface on the flight of 13 March 2007. Photograph courtesy of Juha Karvonen (FIMR).

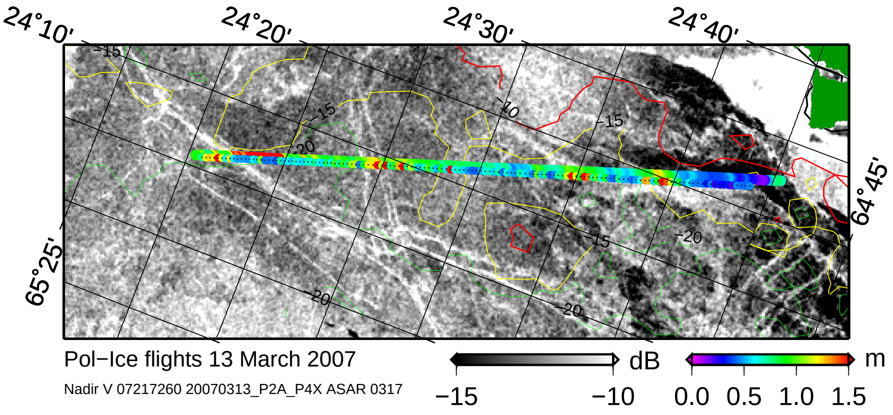

Fig. 5. Flight track of 13 March 2007 and the color coded thickness overlaid on a ASAR WSM image of 17 March 2007. The smaller dots indicate the helicopter EM and the larger dots the SkyVan EMIRAD measurements. The size of the footprints are not in scale. The bathymetry is indicated with the isolines. The island Hailuto is in the upper right corner in green color.

Title Page
Abstract
Introduction
Conclusions
References
Tables
Figures
◀▮
▶▮
◀
▶
Back
Close
Full Screen / Esc
Printer-friendly Version
Interactive Discussion

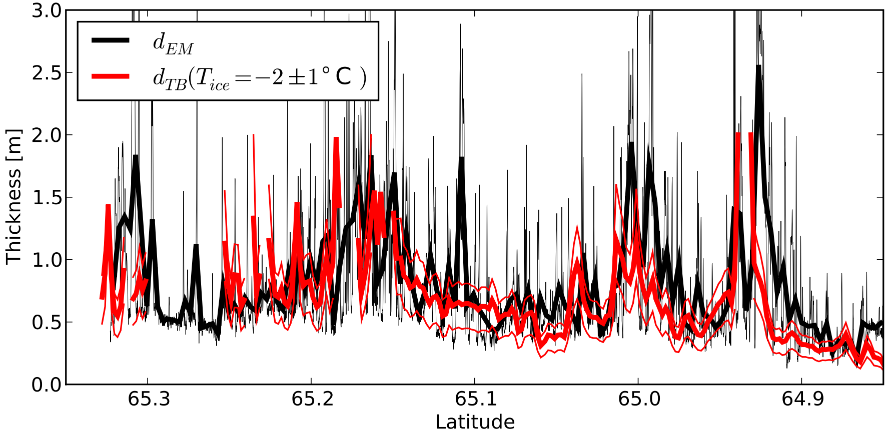

Fig. 6. Thickness retrievals from the flight of 13 March 2007. The graph shows the EM-thickness d_{EM} and the thickness d_{TB} derived from the brightness temperature for the prescribed ice temperature $T_{ice} = -2\pm1^\circ\mathrm{C}$. Data gaps in the red ($d_{\mathrm{TB}}$) curve indicate failures of the retrieval method.

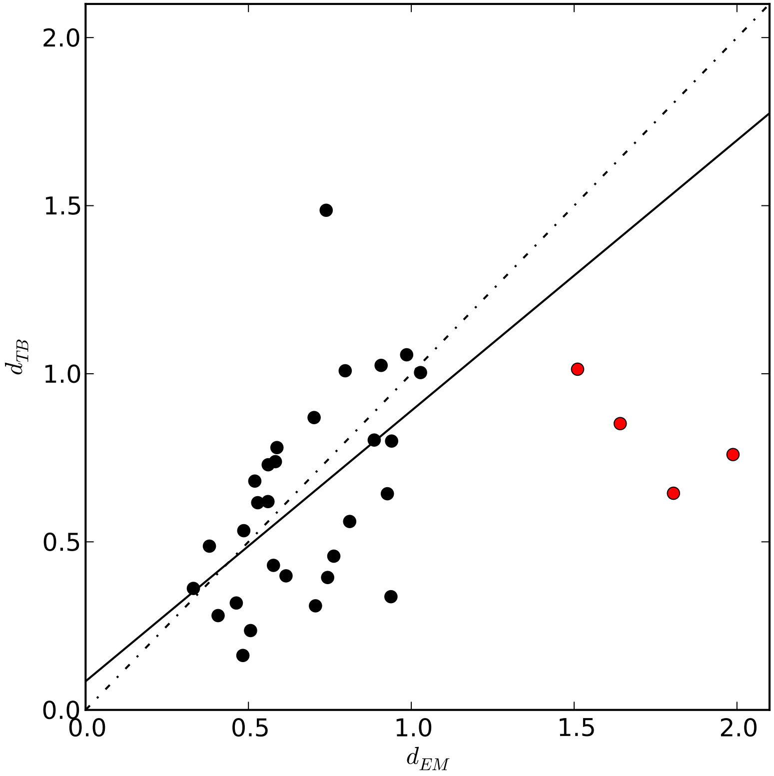

Fig. 7. Scatterplot d_{TB} and d_{EM} for interpolated averages along the track shown in Fig. 6. Each point represents an average over a section of about 1200 m which is similar to the doubled 3 dB footprint of the EMIRAD instrument. A linear regression yield $d_{\mathrm{TB}} = 0.8 d_{\mathrm{EM}} + 0.08$ m with a standard error of 0.16 and a correlation coefficient of $r = 0.5$ by including only the values with $d_{\mathrm{EM}} < 1.5$ m (black dots). The correlation decreases to $r = 0.1$ by including also the values $d_{\mathrm{EM}} > 1.5$ m (red dots).

Title Page
Abstract
Introduction
Conclusions
References
Tables
Figures
◀
▶
Back
Close
Full Screen / Esc
Printer-friendly Version
Interactive Discussion

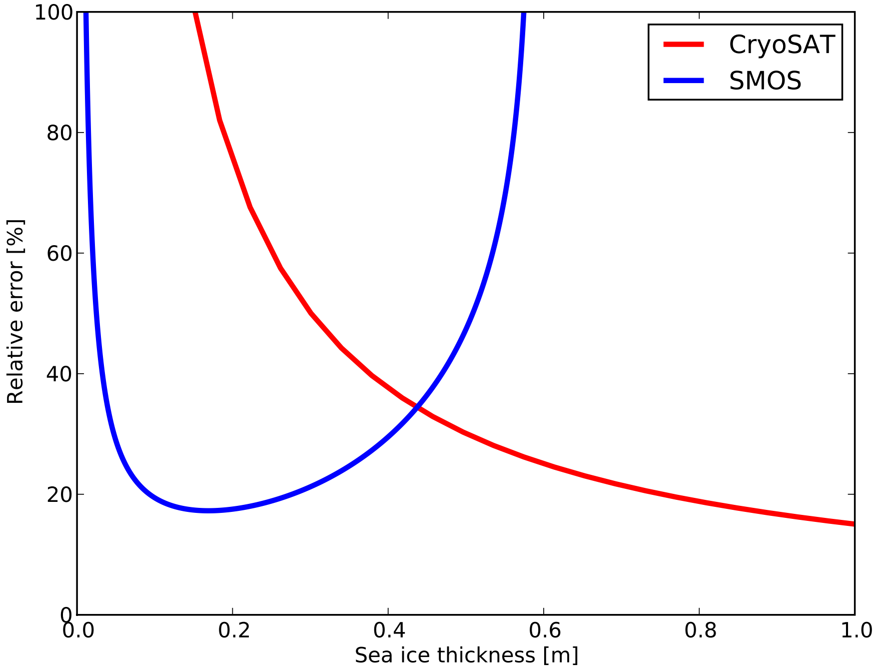

Fig. 8. Error characteristic of SMOS and CryoSat ice thickness retrieval for a simplified error budget as explained in the text.